BIOCHEMISTRY
including biophysical chemistry & molecular biology

Acyl-ACP Substrate Recognition in *Burkholderia mallei* BmaI1 Acyl-Homoserine Lactone Synthase

Aubrey N. Montebello,[†] Ryan M. Brecht,[†] Remington D. Turner,[†] Miranda Ghali,[‡] Xinzhu Pu,[†,§] and Rajesh Nagarajan*,[†]

[†]Department of Chemistry and Biochemistry, Boise State University, 1910 University Drive, Boise, Idaho 83725, United States
[‡]Department of Chemistry, Stetson University, DeLand, Florida 32723, United States

Ⓢ *Supporting Information*

ABSTRACT: The acyl-homoserine lactone (AHL) autoinducer mediated quorum sensing regulates virulence in several pathogenic bacteria. The hallmark of an efficient quorum sensing system relies on the tight specificity in the signal generated by each bacterium. Since AHL signal specificity is derived from the acyl-chain of the acyl-ACP (ACP = acyl carrier protein) substrate, AHL synthase enzymes must recognize and react with the native acyl-ACP with high catalytic efficiency while keeping reaction rates with non-native acyl-ACPs low. The mechanism of acyl-ACP substrate recognition in these enzymes, however, remains elusive. In this study, we investigated differences in catalytic efficiencies for shorter and longer chain acyl-ACP substrates reacting with an octanoyl-homoserine lactone synthase *Burkholderia mallei* BmaI1. With the exception of two-carbon shorter hexanoyl-ACP, the catalytic efficiencies of butyryl-ACP, decanoyl-ACP, and octanoyl-CoA reacting with BmaI1 decreased by greater than 20-fold compared to the native octanoyl-ACP substrate. Furthermore, we also noticed kinetic cooperativity when BmaI1 reacted with non-native acyl-donor substrates. Our kinetic data suggest that non-native acyl-ACP substrates are unable to form a stable and productive BmaI1·acyl-ACP·SAM ternary complex and are thus effectively discriminated by the enzyme. These results offer insights into the molecular basis of substrate recognition for the BmaI1 enzyme.
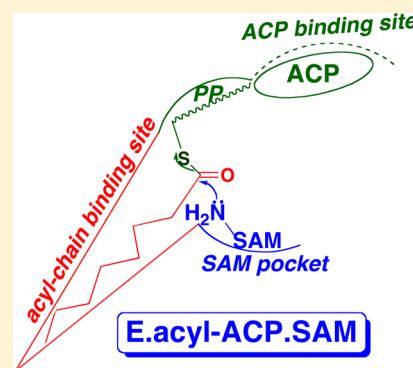
Bacteria communicate by means of small molecules called autoinducers to assess local cell population density through a process known as quorum sensing.[1−3] Gram-negative bacteria use *N*-acyl-homoserine lactone (AHL) mediated quorum sensing to regulate key physiological activities that include virulence, biofilm formation, and toxin production.[4−11] Bacterial AHL synthases belong to the LuxI family of proteins that use acyl-ACP (ACP = acyl carrier protein) and *S*-adenosyl-L-methionine (SAM) to make intracellular AHL autoinducers.[12−19] Since the AHL autoinducers synthesized by a bacterium are species-specific, tight specificity in the native AHL signal synthesized by each bacterium is critical for efficient interbacterial communication. While SAM is a conserved substrate for AHL synthases, specificity in the AHL signal arises from the structure of the acyl chain (short-chain vs long-chain, substituted vs unsubstituted, etc.) in the acyl-ACP substrate.[15−22] In order to achieve tight AHL signal specificity, AHL synthases must be able to selectively recognize the correct acyl-ACP substrate from the cellular acyl-ACP pool to synthesize the native autoinducer. The molecular basis of substrate selectivity in AHL synthases, however, remains poorly understood.

Quorum sensing in *Burkholderia mallei* has been implicated in chronic infections associated with Glanders disease.[23−25] *B. mallei* contains BmaI1-BmaR1 and BmaI3-BmaR3 homologs that make octanoyl homoserine lactone and 3-hydroxyoctanoyl

homoserine lactone autoinducers, respectively.[26,27] In BmaI1-catalyzed octanoyl-homoserine lactone synthesis, the acylation step involves transfer of the fatty acyl group from octanoyl-ACP to the α-amino group in SAM, with cleavage of the acyl-thioester bond to release holo-ACP (Figure 1).[12,14,15] Although SAM is used as a methyl donor in several biological reactions, in AHL synthesis, the 3-amino-3-carboxypropyl group of this substrate is utilized to form a homoserine lactone ring accompanied by release of methylthioadenosine (MTA).[11−16] While the lactone ring is a conserved moiety in acyl homoserine lactones, the specificity in autoinducer signal arises from the acyl-chain of the acyl-ACP substrate.[2,3,14−19] Therefore, to achieve tight AHL signal specificity, BmaI1 must selectively recognize octanoyl-ACP from other non-native (nonspecific) acyl-ACPs in the cellular acyl-ACP pool. If the enzyme were not selective, a non-native acyl-ACP substrate reacting with BmaI1 would result in synthesis of nonspecific acyl-homoserine lactones that would add noise to interbacterial communication. It is therefore imperative for an acyl-homoserine lactone synthase enzyme such as BmaI1 to keep AHL synthesis rates low with nonspecific acyl-ACP substrates. How AHL synthase enzymes achieve this task remains a mystery.
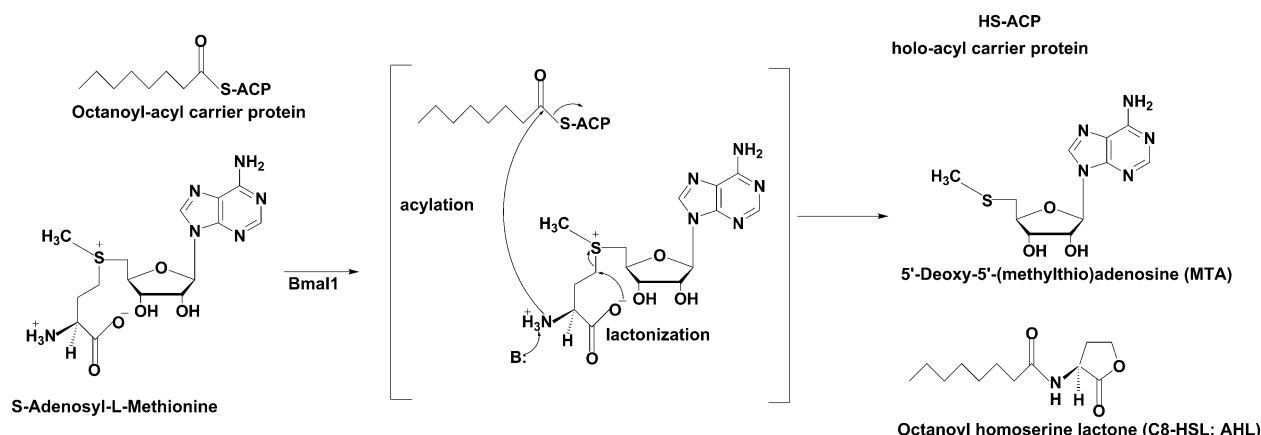
Figure 1. BmaI1 catalyzed AHL synthesis. Octanoyl-ACP (C8ACP) is the acyl-donor, and *S*-adenosyl-L-methionine (SAM) is the acyl-acceptor in this reaction. The lactone moiety in AHL autoinducer is derived from the SAM substrate, and the acyl-chain is obtained from acyl-ACP.
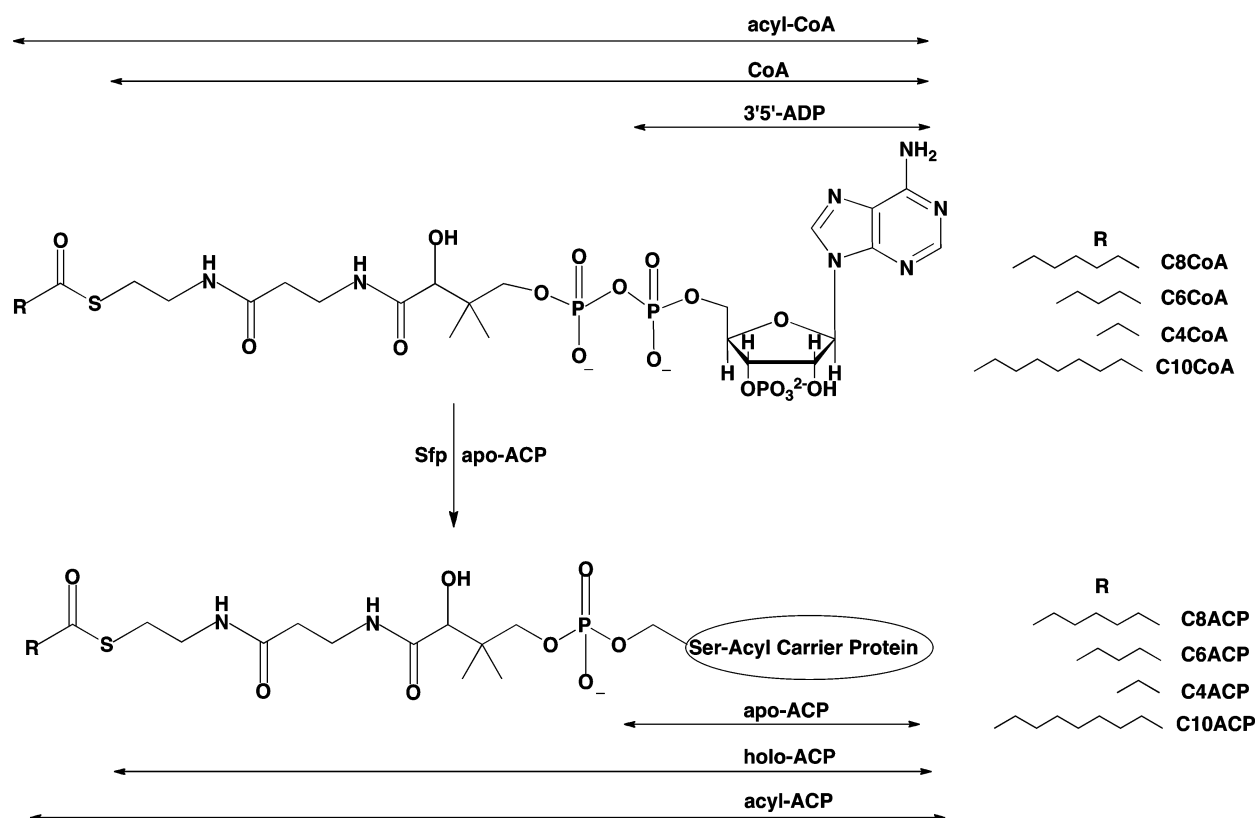

Figure 2. Substrates used in this study. The acyl–acyl carrier protein substrates for BmaI1 was enzymatically synthesized from corresponding acyl-CoA substrates through *Bacillus subtilis* Sfp phosphopantetheinyl transferase. Pantetheine linker connects the acyl-chain to the carrier protein and 3′5′-ADP in acyl-ACP and acyl-CoA, respectively.

To limit buildup of nonspecific signals (noise) during intercellular communication, it is reasonable to assume a model where fatty acid biosynthesis could be modulated to favor accumulation of native acyl-ACPs. Hoang et al. have demonstrated that under certain limiting conditions such as inhibition of the β-keto acyl-ACP reductase enzyme during fatty acid biosynthesis, a long-chain AHL synthase enzyme (LasI) synthesized short-chain AHLs both in vitro and in vivo, probably due to changes in composition of metabolic acyl-ACP pool.[28] Although we cannot rule out the possibility that in vivo metabolic activity might adapt to facilitate accrual of certain acyl-ACPs in response to an environmental need such as quorum sensing, controlling AHL synthesis by modulating fatty

acid biosynthesis alone seems far-fetched. We believe that the specificity in AHL signal synthesis most likely arises from a combination of modulated acyl-ACP pool supply and effective substrate discrimination by AHL synthase enzymes. Although there is some evidence supporting the latter proposition, the extent to which signal synthesis enzymes contribute to achieving tight quorum sensing signal specificity is unknown. To address this long-standing question, we used mechanistic enzymology to investigate how an acyl-homoserine lactone synthase specifically recognizes its native acyl-ACP from non-native acyl-ACP substrates.

X-ray structures of *Pantoea stewartii* EsaI (3-oxohexanoyl-homoserine lactone synthase), *Pseudomonas aeruginosa* LasI (3-

oxododecanoyl-homoserine lactone synthase), and *Burkholderia glumae* TofI (octanoyl-homoserine lactone synthase) reveal a V-shaped hydrophobic cleft that accommodates the acyl-chain of an acyl-ACP substrate.[20−22,29] The amino acids lining the cleft appear to confer specificity to the acyl-chain binding in this pocket.[18,19] For instance, in the 3-oxohexanoyl-homoserine lactone synthase EsaI, the acyl-chain pocket is lined with bulky amino acid side chains restricting the acyl-chain length to six carbons. In the X-ray structure of EsaI and LasI, the acyl-chain pocket carries a threonine residue (Thr140 in EsaI and Thr142/Thr144 in LasI) that could act as specificity determinants between 3-oxoacyl-ACP and unsubstituted acyl-ACP substrate. Mass-spectrometry analysis of AHLs produced in vivo by the EsaI Thr140Ala mutant showed a dramatic increase in unsubstituted hexanoyl homoserine lactone over the native autoinducer, the 3-oxohexanoyl homoserine lactone.[19] Similar results were observed when the Thr142 residue in LasI was mutated to glycine or alanine (although the shift was smaller than with EsaI). Interestingly, when the Thr144 residue in LasI was mutated to valine, multiple AHLs including odd and even chains, saturated and unsaturated, 3-oxo and 3-hydroxyl chains were detected.[19] It is evident from the above studies that amino acids lining the acyl-chain pocket contribute to acyl-chain selectivity. It is not apparent, however, just how this pocket alone can aid acyl-homoserine lactone synthase to select against nonspecific acyl-ACP substrates with only subtle structural variations in the acyl-chain (3-oxo vs 3-hydroxyl, two carbon shorter or longer acyl-chains etc.). Clearly, additional interactions between phosphopantetheine and ACP with the enzyme must also play a significant role in substrate selectivity.

In this paper, we focus our study on the BmaI1 AHL synthase enzyme to address two key questions: (a) What are the differences in rates of AHL synthesis between native and non-native acyl-ACP substrates reacting with BmaI1? (b) How does BmaI1 recognize its native octanoyl-ACP from other non-native, shorter or longer-chain acyl-ACP substrates? Our findings imply that only the native acyl-ACP substrate forms a stable and productive E·acyl-ACP·SAM ternary complex with BmaI1. On the basis of our data, we conclude that formation of a stable and productive E·acyl-ACP·SAM ternary complex is an important contributor to acyl-ACP substrate recognition, which increases the catalytic efficiency of octanoyl-ACP relative to non-native acyl-ACPs reacting with with BmaI1 acyl-homoserine lactone synthase enzyme.

■ MATERIALS AND METHODS

Materials. All acyl-CoA's were purchased from Sigma-Aldrich Chemical Co. or Life Sciences Resources Inc., Milwaukee, WI. All chemicals used for protein purification, enzyme assays, and HPLC solvents were from Sigma-Aldrich or ThermoFisher Scientific. UV−vis data were acquired using a Thermo Scientific Evolution260 spectrophotometer, and HPLC data were obtained using an Accela600 instrument from Thermo Scientific. The molecular mass of ACP and its derivatives were determined using a Bruker maXis quadrupole time-of-flight (Q-TOF) spectrometer. The methylthioadenosine nucleosidase (MTAN) gene was obtained from Dr. Ken Cornell at Boise State University. The plasmid carrying the genes for the *B. mallei* ATCC23344 BmaI1 and *Escherichia coli* DK574-pJT94 ACP were obtained as a generous gift from Dr. Peter Greenberg at the University of Washington, Seattle. The plasmid carrying *Bacillus subtilis* Sfp phosphopantetheinyl

transferase was supplied by Dr. Michael Burkart at the University of California, San Diego.

Protein Purification. BmaI1 was expressed and purified by a minor modification of previously published protocols.[30] Briefly, 2 L of Luria−Bertani broth with 100 μg/mL streptomycin was inoculated with BmaI1 and grown at 37 °C. Expression was then induced at the mid-log phase by addition of 0.5 mM IPTG, cooled to 16 °C, and allowed to express overnight. Growth cultures were then centrifuged at 4500g at 4 °C for 15 min to pellet cells, which were frozen at −80 °C until further use. Frozen pellets were thawed on ice for 45 min prior to lysis. For each liter of growth culture, 2 mL B-PER reagent (Thermo Scientific), 20 μL of DNase and RNase (1 mg/mL) and 25 μL of phenylmethylsulfonyl fluoride (13 mg PMSF in 750 μL isopropyl alcohol) solution were added, followed by incubation at room temperature for 15 min under gentle shaking before being centrifuged at 13000g for 10 min. Purification was achieved via Ni^{2+}-NTA affinity chromatography. The supernatant was loaded on to a Ni^{2+}-NTA column, pre-equilibrated with 0.5 M NaCl in 50 mM Tris-HCl, pH 7.5 (Buffer A), and washed with 10 mL of 50 mM imidazole in buffer A. BmaI1 was eluted from the column using 10 mL of 300 mM imidazole in buffer A. BmaI1 purity was confirmed using SDS-PAGE. Protein concentration was determined using UV−vis measurement (ε_{280} = 29450 M^{-1} cm^{-1}).

Purification of *E. coli* apo-acyl carrier protein (apo-ACP) was accomplished by minor modification of previously published protocols.[30−34] Chemical lysis of cell pellets was achieved with B-PER reagent, as described above. ACP was purified using a Whatman DE52 diaminoethyl cellulose resin. The ACP was precipitated by addition of 0.02% sodium deoxycholate and 5% trichloroacetate, and after 30 min, the pellet was collected by centrifugation and resuspended in 0.5 M Tris-HCl, pH 8.0 buffer. This precipitation step was omitted to prepare unprecipitated apo-ACP. Fractions containing pure protein by SDS-PAGE were desalted using a PD10 column (GE Life Sciences) and concentrated using a 3 kDa MWCO spin filter column.

Acyl-ACPs were prepared from acyl-CoAs and apo-ACP by means of the *B. subtilis* Sfp phosphopantetheinyl transferase enzyme.[30,35,36] The transferase reaction mixture (2 mL) contained 50 mM Tris-HCl pH 6.8, 10 mM magnesium chloride, 750 μM apo-ACP, 937 μM acyl-CoA (1.25× apo-ACP), and 3 μM Sfp. During the preparation of long-chain acyl-ACPs (carbon chain lengths greater than eight), precipitates formed in the reaction mixture prevented the reaction from proceeding to completion. To avoid precipitation, the corresponding long-chain acyl-CoAs were incrementally added to the reaction mixture over 15 min intervals. The transferase reactions were incubated at 37 °C and monitored by UHPLC for completion. Ammonium sulfate at 75% saturation was then added and the reaction mixture was stirred for 1 h at 4 °C to precipitate Sfp. The precipitated Sfp was pelleted by centrifugation at 13000g for 15 min. For preparation of precipitated acyl-ACP, the reaction mixture was precipitated with two volumes of acetone overnight at −20 °C, resuspended in 15 mL of 25 mM Tris-HCl, pH 7.5, and desalted with a 3 kDa MWCO spin filter column. The acetone precipitation step was omitted to prepare unprecipitated acyl-ACPs.

Molecular Mass Determination. The molecular masses of ACP and its derivatives were determined using a Bruker maXis quadrupole-time-of-flight (Q-TOF) mass spectrometer equip-
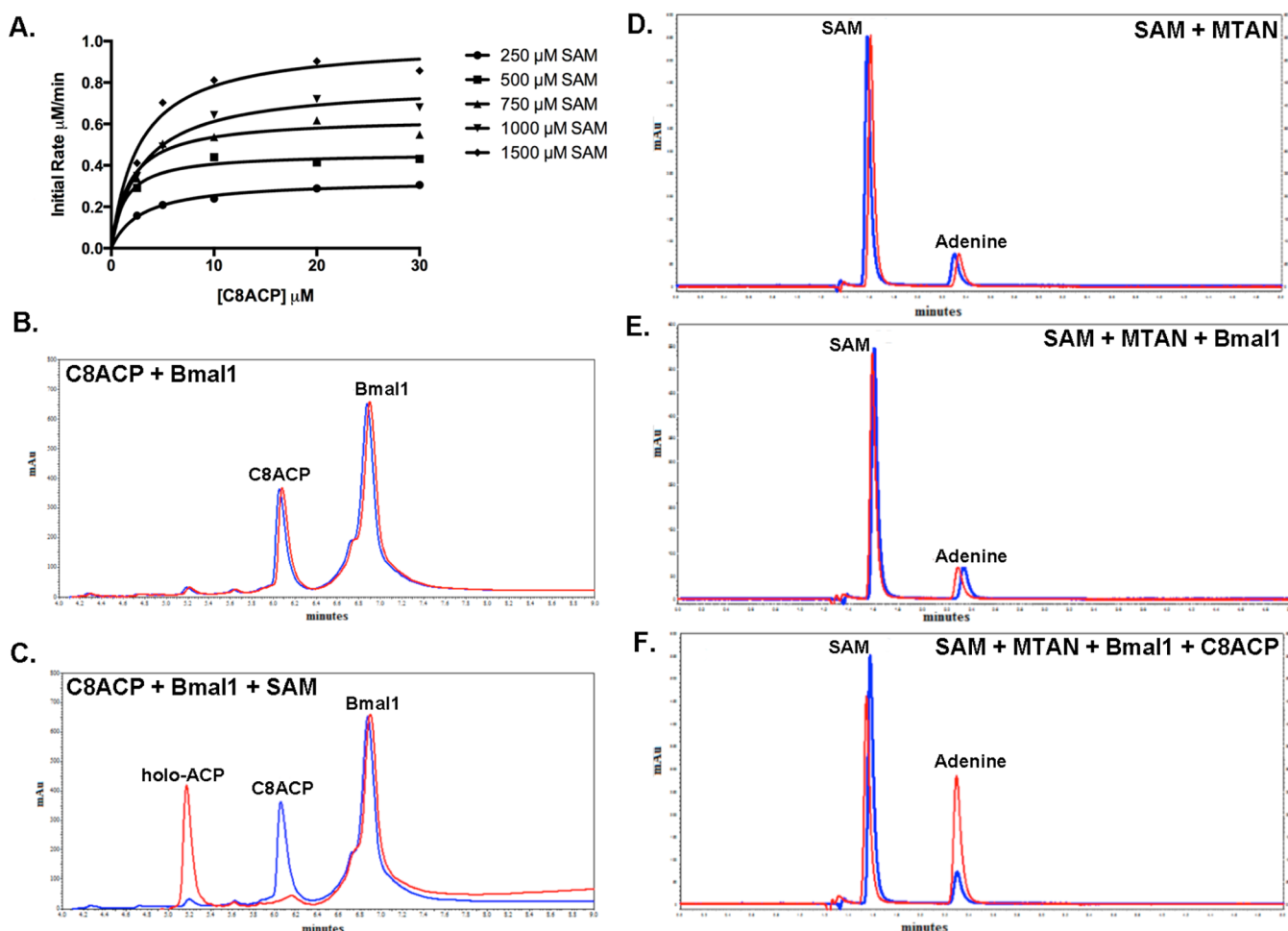
Figure 3. Mechanism of substrate addition in BmaI1. (A) Octanoyl-ACP and SAM substrate-velocity data fit to a sequential equation (eq 1 in main text). Since the data fitted equally well to the ping-pong equation, an independent HPLC-based experiment was conducted to distinguish between these two mechanistic possibilities. Panels B−F refer to HPLC experiments that tested for the ping-pong mechanism of substrate addition in BmaI1. (B) HPLC chromatogram for 40 μM C8ACP (octanoyl-ACP) incubating with 40 μM BmaI1 at 30 min (blue) and 60 min (red). Holo-ACP was not released when SAM was excluded from reaction mixture. (C) Holo-ACP release monitored after 30 min incubation of reaction mixture 'B' with 1.2 mM SAM-chloride (red). When SAM is included in the reaction mixture, acylation occurred as seen by the decrease in C8ACP peak area with a concomitant increase in the holo-ACP peak area. (D) Control reaction for incubation of 100 μM SAM with 1.6 μM methylthioadenosine nucleosidase (MTAN). S-Adenosylhomocysteine (SAH) and methylthioadenosine (MTA) impurities in SAM commercial sample react with MTAN to release adenine. Since adenine has a higher extinction coefficient at 260 nm than methylthioadenosine (MTA), MTAN was included in this assay. SAM and MTAN incubation was monitored at 5 min (blue) and 45 min (red). (E) BmaI1 addition to the reaction mixture D (SAM + MTAN). Twenty micromolar BmaI1 was added to reaction mixture D that was preincubated for 45 min. The chromatogram was monitored after 60 min of enzyme addition (red). There is no change in peak area for SAM and adenine, suggesting no reaction occurred between SAM and BmaI1. (F) Addition of 60 μM C8ACP to the reaction mixture E (SAM + MTAN + BmaI1). Chromatogram monitored after 80 min (red) of octanoyl-ACP addition revealed an increase in adenine peak area with a concomitant decrease in SAM peak area. BmaI1 reacting with C8ACP and SAM release MTA, which reacts with MTAN coupling enzyme to release adenine. Therefore, lactonization reaction is dependent on addition of C8ACP substrate excluding a ping-pong mechanism for BmaI1.

ped with electrospray ionization (ESI). Ten microliters of samples were injected onto a Phenomenex C18 column (100 × 2.1 mm, 2.6 μ) followed by a simple linear gradient for sample desalting and separation. The initial eluent was 98% mobile phase A (99.9% water, 0.1% formic acid) and 2% B (99.9% acetonitrile, 0.1% formic acid) for 5 min, and then mobile phase B was increased to 50% over 25 min. The LC eluent was diverted to waste during the first 5 min of the gradient to eliminate salts in the sample buffer. Mass analysis was performed using the positive ion mode with a spray voltage of 4000 V. The obtained mass spectra were deconvoluted using Bruker Data Analysis 4.0 software. ACP: calculated mass 8508.3 Da, observed mass 8507.5 Da; C4ACP: calculated mass 8916.8 Da, observed mass 8918.2 Da; C6ACP: calculated mass 8944.9

Da, observed mass 8946.2 Da; C8ACP: calculated mass 8973.0 Da, observed mass 8974.4 Da; C10ACP: calculated mass 9000.8 Da, observed mass 9002.3 Da.

Bmal1 Assays. The enzymatic reaction catalyzed by BmaI1 was monitored using a colorimetric assay that is sensitive to the free holo-ACP thiol generated at the acylation step in AHL synthesis.[15,16] A typical reaction contained 30 μM dichlorophenolindophenol (DCPIP) and 100 mM HEPES, pH 7.2. C8ACP was varied between 2.5 and 40 μM, and SAM was varied between 250 and 1500 μM. The initial rates were fit to the Cleland SEQUEN program (eq 1) to estimate kinetic constants.[37] To estimate Michaelis constants for nonspecific acyl-ACPs, SAM was fixed at 3 or 6 mM, while the acyl-ACP concentrations varied from 5 to 100 μM. To estimate the K_m

Table 1. Precipitation Effects on Acyl-ACP Substrate Activity

apo-ACP precipitation	acyl-ACP[a] precipitation	k_{cat} (s^{-1})	K_m (μM)	k_{cat}/K_m (M^{-1}) (s^{-1})	k_{cat}/K_m relative[b]
yes	no	0.096 ± 0.010	6 ± 1	$(1.6 \pm 0.3) \times 10^4$	1
yes	yes	0.062 ± 0.003	11 ± 3	$(0.56 \pm 0.15) \times 10^4$	0.35
no	no	0.076 ± 0.008	30 ± 6	$(0.26 \pm 0.06) \times 10^4$	0.16

[a]SAM is the fixed substrate. [b]$[\{k_{cat}/K_m\}^{acyl\text{-}ACP}/\{1.6 \times 10^4\}]$.

value of SAM, acyl-ACP was maintained at 4−10× the acyl-ACP's K_m. The nonenzymatic, background rates with DCPIP increased in proportion with an increase in SAM concentration. In addition, we also observed a smaller increase in background rates with DCPIP when acyl-ACP concentration was increased. To minimize background rates, SAM concentration was capped between 3 and 6 mM. Since fixed substrates may not be under true saturating conditions, both Michaelis constants and turnover number determined in this study must be interpreted as apparent kinetic constants. Prior to enzyme addition, both SAM and acyl-ACP substrates were incubated with DCPIP in the assay buffer for 10 min or longer until background rates become negligible. Reactions were then initiated by the addition of BmaI1 (0.24, 0.56, 1.0, 2.0, 5.0 μM for octanoyl-ACP, hexanoyl-ACP, decanoyl-ACP, butyryl-ACP, and octanoyl-CoA respectively). The thiol-dependent reduction of DCPIP was monitored at 600 nm (ε_{600} = 21000 M^{-1} cm^{-1}) over 15 min. The initial rate data were fit to the Michaelis−Menten or a substrate inhibition equation (eq 2) using GraphPad Prism 6.0. All experiments were done in triplicate to check for reproducibility and to estimate errors.

$$v_o = \frac{V_{max}[A][B]}{K_{ia}K_m^B + K_m^B[A] + K_m^A[B] + [A][B]} \quad (1)$$

$$v_o = \frac{V_{max}[A]}{K_m^A + [A]\left(1 + \frac{[A]}{K_i}\right)} \quad (2)$$

$$v_o = \frac{V_{max}[A][B]}{K_m^B[A] + K_m^A[B] + [A][B]} \quad (3)$$

$$v_o = \frac{V_{max}[A]^n}{K_{0.5}^n + [A]^n} \quad (4)$$

For substrates that displayed nonhyperbolic rate curve behavior, the substrate−velocity data were fitted to eq 4. The $K_{0.5}$ value determined from data fit is assumed to reflect the apparent Michaelis constant (K_m) for the substrate.

HPLC Assay. To monitor holo-ACP by HPLC, we used a gradient beginning at 75% solvent A and ending with 25% A over a 10 min period at a flow rate of 600 μL/min. To monitor MTA, the gradient began at 0% B and ended at 30% B over a 10 min interval. The flow rate was maintained at 500 μL/min. Solvent A is 0.1% TFA in nanopure water, and solvent B is 0.1% TFA in acetonitrile. To test for the acylation reaction, 40 μM octanoyl-ACP and 40 μM BmaI1 enzyme were incubated at room temperature for 60 min in 100 mM HEPES buffer pH 7.2. After 60 min, 1.2 mM SAM-chloride (Sigma) was added to the reaction mixture, which was allowed to incubate for an additional 30 min before being injected onto the HPLC. The reaction was monitored for BmaI1 dependent holo-ACP release (Figure 3). To test for the lactonization reaction, a mixture of SAM chloride, methylthioadenosine nucleosidase (MTAN), and BmaI1 was incubated at concentrations of 100 μM, 1.6 μM,

and 20 μM respectively. A control experiment was also performed with only 100 μM SAM chloride. Both the reaction and control were incubated for 1 h. 60 μM C8ACP was then added to the reaction mixture, and adenine release by {BmaI1-MTAN} enzyme couple was monitored as described above (Figure 3).

■ **RESULTS AND DISCUSSION**

Precipitation Affects Acyl-ACP Activity. Phosphopantetheinyl transferase (Sfp) catalyzes reaction of octanoyl-CoA (C8CoA) with apo-ACP yielding octanoyl-ACP (C8ACP). Three different methods were used to prepare octanoyl-ACP: (a) apo-ACP precipitated and octanoyl-ACP unprecipitated, (b) both apo-ACP and octanoyl-ACP precipitated, and (c) both apo-ACP and octanoyl-ACP unprecipitated. To purify apo, holo and acyl-ACPs, some laboratories precipitated the acyl carrier protein while others did not.[38−44] Since we noticed significant variations in how ACPs were purified among these laboratories, we asked if precipitating apo-ACP or acyl-ACP would affect acyl-substrate activity with acyl-homoserine lactone synthase, BmaI1? Indeed, we observed that BmaI1 activity is sensitive to apo and acyl-ACP precipitation. Interestingly, we observed substrate inhibition only for precipitated apo-ACP and unprecipitated octanoyl-ACP (method "a" above), which was also the most-active substrate in this series. To check if these observations could arise from experimental artifacts in our assay conditions, we compared the activity of precipitated apo-ACP and precipitated octanoyl-ACP substrate with BmaI1 with a previously published report from Greenberg's laboratory.[30] The k_{cat} and K_m and the kinetic response for precipitated octanoyl-ACP with BmaI1 are in-line with findings from Greenberg's laboratory, which reassures us that our kinetic observations are real and would most likely be reproducible at other laboratories.[30] Although acyl-ACP precipitation resulted in a 3-fold decrease in substrate activity with BmaI1, we were unable to see any noticeable difference between precipitated and unprecipitated acyl-ACP in conformationally sensitive (native) gel electrophoresis (Table 1). From these results, one must conclude that if acetone precipitation altered acyl-ACP tertiary structure, it must be subtle and undetected by native gel electrophoresis. Our kinetic data reveal that acyl-ACP substrate activity with BmaI1 is sensitive to protein precipitation (Figure 4, Table 1).

Octanoyl-ACP and SAM Substrates Add in Sequential Order to BmaI1. The substrate velocity data for octanoyl-ACP and SAM reacting with BmaI1 fit well to both sequential and ping-pong equations (eqs 1 and 3).[37,45−47] In order to distinguish between these two mechanisms, we resorted to HPLC. If substrate addition followed a ping-pong mechanism, we should observe release of one of the products (holo-ACP, MTA, C8-HSL) before the second substrate reacted with the enzyme. Therefore, we sought to check if a BmaI1−octanoyl−ACP mixture could release holo-ACP in the absence of SAM (acylation reaction) and if a BmaI1−SAM mixture could release MTA in the absence of octanoyl-ACP (lactonization reaction).
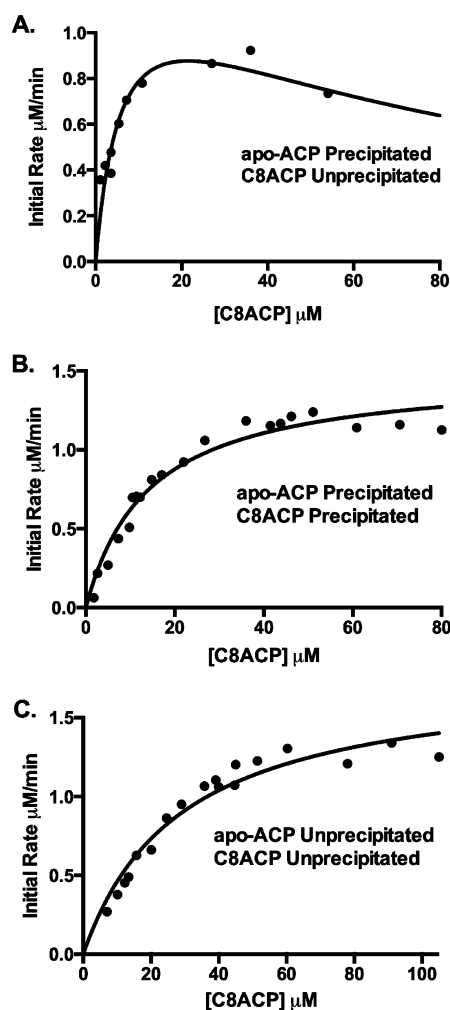
Figure 4. Apo-ACP and acyl-ACP precipitation on BmaI1 activity. Substrate—velocity curves for (A) apo-ACP precipitated, octanoyl-ACP unprecipitated, (B) both apo-ACP and octanoyl-ACP precipitated, (C) both apo-ACP and octanoyl-ACP unprecipitated substrates. Each experiment was conducted in triplicate and the rates were averaged. SAM concentration was fixed at 3 mM, and BmaI1 concentration was maintained at 0.24 μM (A) or 0.40 μM (B and C) in these experiments. The most active octanoyl-ACP sample was obtained when the precipitation step was included in apo-ACP and omitted from acyl-ACP purification.

If octanoyl-ACP reacted first with BmaI1 via ping-pong mechanism, then an active site nucleophile could release holo-ACP resulting in an acyl-enzyme complex. SAM could then react with the acyl-enzyme complex to complete the acylation step. Alternatively, if lactonization occurred prior to binding of octanoyl-ACP substrate to BmaI1, we should observe MTA release even if acyl-ACP is excluded from the reaction. However, we did not observe the release of either holo-ACP or MTA unless both substrates were added to the reaction mixture. Therefore, this result excludes the ping-pong mechanism of substrate addition to BmaI1. Interestingly, when the substrate—velocity data were fitted to a sequential equation, we found that the substrate dissociation constant for the first substrate (K_{ia}) was 125 $\pm$ 43 nM. It was then apparent that the magnitude of the $K_{ia}*K_m^B$ term in the denominator for the sequential substrate—velocity equation (eq 1) is smaller compared to ($K_m^A[B] + K_m^B[A] + [A][B]$). Therefore, under these conditions, a sequential substrate—velocity equation would resemble a ping-pong equation (compare eqs 1 and 3), which is probably why our data fit equally well to both eqs 1 and 3?

To determine whether substrate addition is ordered or random, we attempted to conduct product inhibition studies with BmaI1. The low K_{ia} value suggested that the first substrate binds tightly to the enzyme ($k_{on} \gg k_{off}$). Therefore, the mechanism of substrate addition must either follow an ordered sequential or a preferred-ordered random sequential pathway, where acyl-ACP is most likely the first substrate to add to the enzyme (K_m of acyl-ACP is much lower than K_m of SAM). This is contrary to the well-studied RhlI enzyme, where butyryl-ACP and SAM substrates follow an ordered sequential path with SAM substrate binding first to the enzyme.[14] In BmaI1, if acyl-ACP is the first substrate to add to the enzyme, then the last product released should inhibit BmaI1 in a competitive manner under varying acyl-ACP substrate and nonsaturating, fixed SAM conditions. Furthermore, when the fixed SAM concentration was kept around its K_m value and acyl-ACP substrate was varied, we should observe noncompetitive and uncompetitive inhibition with BmaI1 for first and second products, respectively. Nonetheless, a thiol-sensitive DCPIP assay was unsuited to measure holo-ACP inhibition. In addition, weak inhibition observed with MTA and solubility issues with octanoyl homoserine lactone in the enzyme assay buffer precluded us from conducting product inhibition studies with BmaI1.

Catalytic Efficiencies for Nonspecific Acyl-Donor Substrates. Nonspecific acyl-ACPs are less active compared to the native octanoyl-ACP (C8ACP) in reaction with BmaI1 (Table 2). The increase in K_m was smaller compared to the decrease in k_{cat}. Among the nonspecific acyl-ACP substrates tested, hexanoyl-ACP (C6ACP) was the most active substrate with BmaI1. The catalytic efficiencies for butyryl-ACP (C4ACP) and decanoyl-ACP (C10ACP) decreased more than 20-fold compared to octanoyl-ACP. For octanoyl-CoA (C8CoA), however, both k_{cat} and K_m values were severely affected (Table 2). The 5000-fold decrease in catalytic efficiency for octanoyl-CoA relative to octanoyl-ACP indicates ACP contributes significantly to substrate activity (Table 2). Furthermore, we found that 3′5′-ADP inhibited BmaI1 with a

Table 2. Acyl-ACP Substrate Specificity

variable S	fixed S	k_{cat} (s^{-1})	K_m μM	k_{cat}/K_m (M^{-1}) (s^{-1})	k_{cat}/K_m relative[b]
C8ACP[a]	SAM-Cl	0.096 $\pm$ 0.010	6 $\pm$ 1	(1.6 $\pm$ 0.3) $\times$ 10^4	1.00
C6ACP[a]	SAM-Cl	0.025 $\pm$ 0.002	4 $\pm$ 1	(0.63 $\pm$ 0.16) $\times$ 10^4	0.38
C4ACP[a]	SAM-Cl	0.010 $\pm$ 0.001	29 $\pm$ 2	(3.4 $\pm$ 0.4) $\times$ 10^2	0.02
C10ACP[a]	SAM-Cl	0.015 $\pm$ 0.002	19 $\pm$ 4	(7.9 $\pm$ 0.2) $\times$ 10^2	0.05
C8CoA	SAM-Cl	0.002 $\pm$ 0.0002	541 $\pm$ 14	3.4 $\pm$ 0.3	0.0002

[a]Apo-ACP precipitated, acyl-ACP unprecipitated. [b][{k_{cat}/K_m}$^{acyl-ACP}$/{1.6 $\times$ 10^4}].

Table 3. Effect of Nonspecific Acyl-ACP Substrates on SAM Activity

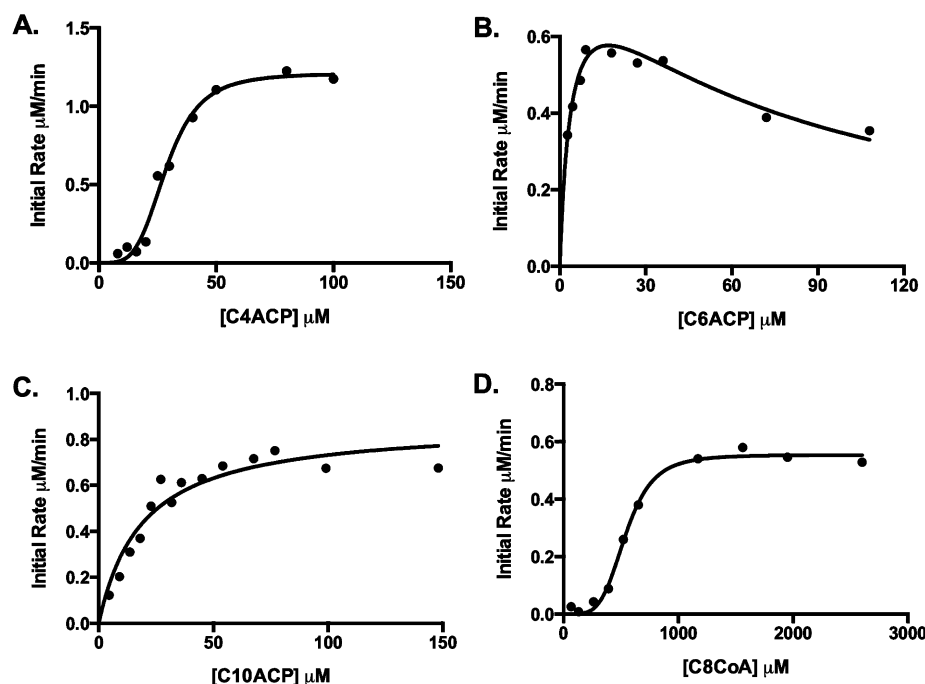| variable S	fixed S	k_{cat} (s^{-1})	K_m (mM)	k_{cat}/K_m (M^{-1}) (s^{-1})	k_{cat}/K_m relative^a
SAM-Cl	C8ACP	0.096 ± 0.010	1.80 ± 0.50	54 ± 16	1.00
SAM-Cl	C6ACP	0.028 ± 0.002	0.54 ± 0.07	52 ± 7	0.98
SAM-Cl	C4ACP	0.018 ± 0.003	1.91 ± 0.32	10 ± 2	0.18
SAM-Cl	C10ACP	0.007 ± 0.001	0.80 ± 0.08	8 ± 1	0.16
SAM-Cl	C8CoA	0.003 ± 0.0002	0.94 ± 0.08	3 ± 0.2	0.05

^{a}[{k_{cat}/K_m}/{54}].

Figure 5. Substrate−velocity curves for nonspecific acyl-ACP substrates reacting with BmaI1. Initial rate as a function of substrate concentration for 3 mM SAM chloride (fixed) and (A) varying butyryl-ACP in 2 μM BmaI1, (B) varying hexanoyl-ACP in 0.56 μM BmaI1, (C) varying decanoyl-ACP in 1 μM BmaI1, and (D) varying octanoyl-CoA in 5 μM BmaI1. Each data point was repeated in triplicate, and the average rate was reported in these graphs. We used higher concentrations of enzyme for assaying poor substrates to obtain comparable rates between assays. The rate curves were sigmoidal for poor substrates (butyryl-ACP, octanoyl-CoA) and hyperbolic for hexanoyl-ACP and decanoyl-ACP substrates. The dissociation constant for hexanoyl-ACP substrate inhibition is 69 ± 14 μM. Deviations from Michaelis−Menten behavior for butyryl-ACP and octanoyl-CoA are indicative of kinetic cooperativity. Positive cooperativity (Hill slope > 1) was observed for both of these substrates. Acyl-ACP substrates were enzymatically synthesized from apo-ACP and acyl-CoA. While apo-ACP was precipitated, all acyl-ACP samples (C4ACP, C6ACP, and C10ACP) were prepared by omitting the acetone precipitation step in substrate purification.

half-maximal inhibitory concentration (IC50) greater than 1.5 mM. The weak affinity of the nucleotide moiety to BmaI1 suggests that the enzyme does not actively discriminate against 3′5′-ADP. Our results are in-line with in vivo observations where wild-type *B. mallei* is known to make three acyl-HSLs, namely, octanoyl-homoserine lactone, hexanoyl-homoserine lactone (both made by BmaI1), and 3-hydroxyoctanoyl-homoserine lactone synthesized by BmaI3 AHL synthase.[25]

The Michaelis constant for SAM was less affected when the fixed substrate was a non-native acyl-ACP substrate (Table 3). SAM substrate catalytic efficiencies decreased in the following order when the fixed acyl-donor substrate was C8ACP > C6ACP > C10ACP, C4ACP > C8CoA. However, the magnitude of decrease in k_{cat}/K_m with varying SAM was lower than that from varying acyl-ACP (Table 3).

Substrate Velocity Curves for Nonspecific Acyl-Donor Substrates. We noticed differences in kinetic responses between good and poor acyl-ACP substrates reacting with BmaI1. In this study, based on the k_{cat}/K_m values, we consider octanoyl-ACP and hexanoyl-ACP as good substrates, while

butyryl-ACP, decanoyl-ACP, and octanoyl-CoA are collectively grouped as poor substrates (Tables 2 and 3). Irrespective of the varying substrate (SAM or acyl-ACP), the overall pattern in substrate-velocity curves was hyperbolic for good substrates and sigmoidal for poor substrates (Figures 5 and 6). Sigmoidal or nonhyperbolic response in rate curves is usually indicative of kinetic cooperativity.[48−60] Moreover, substrates with higher k_{cat}/K_m also displayed substrate inhibition characteristics (Figures 4 and 5). The implications of nonhyperbolic substrate velocity behavior for poor substrates and substrate inhibition for good substrates on mechanism of BmaI1 catalyzed AHL synthesis are discussed below.

Mechanism of Acyl-ACP Substrate Recognition. BmaI1 reacting with a nonspecific acyl-ACP substrate will synthesize a nonspecific AHL autoinducer. In order to achieve higher specificity in signal synthesis, it is imperative for an AHL synthase enzyme like BmaI1 to keep rates with non-native substrates low. To put this in simple terms, BmaI1 should be able to selectively recognize native acyl-ACP from non-native acyl-ACPs in the cytosol to achieve tight signal specificity.
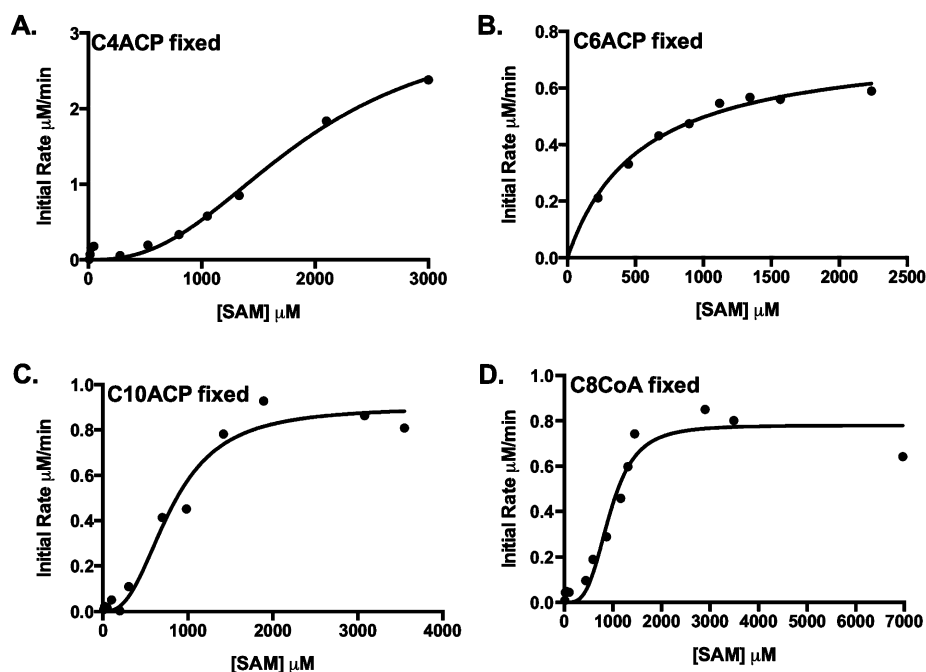
Figure 6. Substrate−velocity curves for SAM. (A−D) Rate curves for SAM when the fixed substrate was 150 μM butyryl-ACP, 38 μM hexanoyl-ACP, 36 μM decanoyl-ACP, and 522 μM octanoyl-CoA respectively. Although apo-ACP was precipitated and resuspended, the precipitation step was omitted during preparation of acyl-ACP (fixed) substrates used in this study. The enzyme concentrations were varied from 0.5 to 5 μM depending on the acyl-ACP substrate used in the experiment. The data points for rate-curves came from an average of triplicate measurements.

Scheme 1. Substrates Add in Random Order to BmaI1[a]
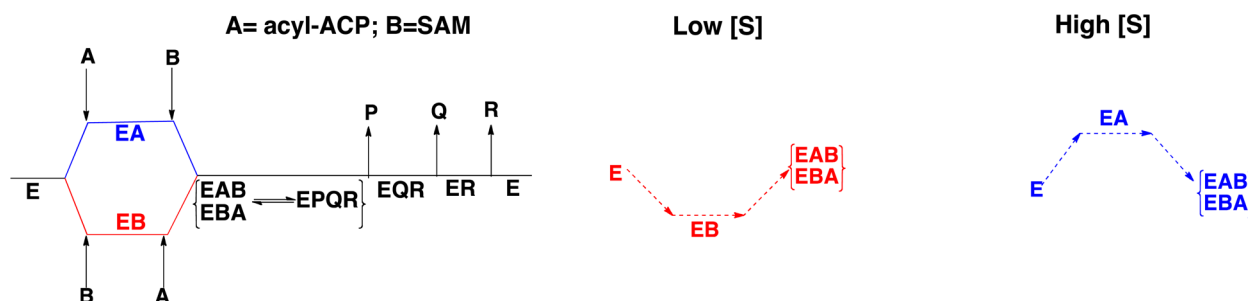
[a]Substrates A and B correspond to acyl-ACP and SAM, respectively. The path highlighted in blue is kinetically favored and red is disfavored. The pathway for non-native acyl-ACP substrate turnover under low and high substrate concentrations is described in this scheme.

Indeed, we noticed differences in kinetic responses and rates between native and non-native acyl-ACP substrates reacting with BmaI1. We observed hyperbolic kinetic response and substrate inhibition for good substrates and non-Michaelis−Menten kinetic response for poor substrates. Substrate inhibition could arise when two substrate molecules bind to the enzyme to form an ES$_2$ complex or the enzyme undergoes slow isomerization.[48] Furthermore, random addition of substrates to a bisubstrate enzyme could also give rise to substrate inhibition.[49,51,60] Sigmoidal substrate−velocity curves observed for poor substrates suggest kinetic cooperativity involving random order substrate addition or a hysteretic or mnemonic enzyme. To the best of our knowledge, oligomerization of acyl-homoserine lactone synthase enzymes has never been detected. The models described below assume a monomeric state for active, BmaI1 AHL synthase enzyme.

Random Addition of Substrates. In a random mechanism, either substrate could add to free enzyme to form E·acyl-ACP (EA) and E·SAM (EB) complexes (Scheme 1). Although

the acyl-ACP substrate could bind to either E or E·SAM complex, the low K_{ia} value for octanoyl-ACP suggests that acyl-ACP must bind more tightly to the free enzyme "E" form. If substrates add in a random fashion, the path where acyl-ACP binds as the first substrate should be favored over SAM binding first to the free enzyme. Hence, we see this case as an example of a preferred-order random mechanism. If this is true, then good substrates such as octanoyl-ACP will bind to "E" populating the kinetically favored pathway (E ⇌ E·octanoyl-ACP ⇌ E·octanoyl-ACP·SAM; top pathway in Scheme 1). This model assumes an [E·SAM·octanoyl-ACP] ternary complex formed in the bottom pathway is less productive or nonproductive, and the resultant steady-state rate is the sum of rates from both of these pathways. When SAM is held constant and octanoyl-ACP concentration is increased from low to high values, more acyl-ACP will bind to the E.SAM complex gradually shifting the reaction toward the disfavored pathway thereby decreasing the overall steady-state rates (Figure 5). Under fixed octanoyl-ACP conditions, however,

BmaI1 must predominantly exist as E·octanoyl-ACP complex (K_{ia} is 125 nM). SAM binds to this complex, and the reaction follows the kinetically preferred pathway. If this model is valid, we must see a hyperbolic rate curve for varying SAM, and indeed this is our observation. The moderately active two-carbon shorter hexanoyl-ACP also falls into this category.

For a poor substrate such as butyrylACP or octanoyl-CoA, E·butyryl-ACP or E·octanoyl-CoA complex is less stable favoring E $\rightleftharpoons$ E·butyryl-ACP or E $\rightleftharpoons$ E·octanoyl-CoA equilibrium toward free enzyme, E. SAM can then bind to E to form E·SAM. As the concentration of butyryl-ACP or octanoyl-CoA is steadily increased from low to high values, the acyl-ACP or acyl-CoA substrate will first bind to E·SAM, which exists at higher concentrations, to form a nonproductive [E·SAM·butyryl-ACP] or [E·SAM·octanoyl-CoA] ternary complex (bottom pathway in Scheme 1). Therefore, rates do not increase with an increase in acyl-substrate concentration, accounting for the lag-phase in the substrate-velocity curve. At higher butyryl-ACP or octanoyl-CoA concentrations, however, more of the acyl-donor substrate would bind to E shifting the AHL synthesis reaction coordinate toward the kinetically preferred pathway leading to the upward increase in the substrate−velocity curve (top pathway in Scheme 1, Figure 5A,D). The only exception is decanoyl-ACP, which shows hyperbolic behavior (Figure 5C). The lack of a lag-phase at low decanoyl-ACP concentrations suggests that AHL synthesis proceeds via the preferred pathway. Therefore, according to this model, the E·decanoyl-ACP complex should be relatively more stable (decanoyl acyl-chain is only two carbons longer than octanoyl acyl-chain) compared to E·butyryl-ACP or E·octanoyl-CoA complexes. The [E·decanoyl-ACP·SAM] ternary complex, however, may not be in a productive conformation, thus decreasing k_{cat} and catalytic efficiency for this substrate. We also find that when SAM is the varied substrate, the rate curves were nonhyperbolic at fixed concentrations of butyryl-ACP, decanoyl-ACP, and octanoyl-CoA (Figure 6). For these poor substrates, E·acyl-ACP (or E·octanoyl-CoA) should be less stable, and therefore E·acyl-ACP $\rightleftharpoons$ E should favor E. Therefore, at low concentrations, SAM binds to E (which is present in excess relative to E·acyl-ACP) to form E·SAM populating the kinetically disfavored pathway accounting for the lag phase in the substrate−velocity curve (Scheme 1). Alternatively, [E·acyl-ACP·SAM] could be unreactive at low SAM concentrations. When SAM concentration is high, the reaction proceeds via the kinetically favored pathway causing the upward lift in the rate-curve. As discussed above, both good and poor substrates fit the preferred-order, random mechanism model. The relative distribution between favored and disfavored paths for substrate addition will depend on the type of acyl-ACP substrate reacting with BmaI1.

Alternative Possibilities. Although a random addition of substrate model provides a rationale to understand kinetic cooperativity observed for non-native substrates reacting with BmaI, other models that could potentially fit our collected data are considered below.[49−61]

1. Acyl-Carrier Protein Existing in Multiple Conformations. Although this model could provide a reasonable explanation for kinetic cooperativity observed for some substrates, we think this scenario is less likely because octanoyl-CoA, a nonprotein based substrate, displays nonhyperbolic kinetics, while the rate curve for decanoyl-ACP, an ACP based poor substrate, is hyperbolic. These results suggest that the cooperative behavior observed for some of these substrates most likely arises from acyl-ACP

binding to more than one *enzyme species* (such as E and E·SAM).

2. Slow Conformational Transition between Multiple Free Enzyme Species in Solution As Observed in a Hysteretic or Mnemonic Enzyme. Enzyme hysteresis is often accompanied by a lag or burst in substrate utilization. A closer look at our progress curves, however, did not reveal lag or burst phases in the time scale of our steady-state assay conditions. Since we do not have any substantial evidence yet to support the existence of more than one free enzyme species (like E and E*) in solution, we have to assume that random addition of substrates model best supports our current data.

CONCLUSIONS

Our data suggest that the rate curves for substrates with low k_{cat}/K_m show cooperative behavior, while others display a standard Michaelis−Menten response. While alternate possibilities discussed above could potentially explain cooperative kinetics observed for non-native acyl-ACPs in reaction with BmaI1, *our best evidence so far* supports a model involving random addition of substrates with acyl-ACP binding first to the free enzyme (top pathway in Scheme 1) more kinetically preferred over SAM binding first to the enzyme (bottom pathway in Scheme 1). For poor substrates, the lag phase observed in the rate curves at low substrate concentrations suggests that catalytic turnover either goes through a less-productive (kinetically disfavored) path or forms an abortive complex. For substrates with higher k_{cat}/K_m (octanoyl-ACP and hexanoyl-ACP), substrate inhibition is observed at saturating concentrations. Although a simplistic model for substrate inhibition proposes binding of two substrate molecules to an enzyme to form an ES$_2$ complex, in many instances, however, substrate inhibition involves a more complex mechanism that includes slow-transition between multiple enzyme species in solution.[48] Nonetheless, we do not have any evidence yet to support the existence of an ES$_2$ complex. However, on the basis of our current data, we can infer that positive cooperativity observed for poor substrates and substrate inhibition seen for good substrates lends support to the hypothesis that acyl-ACP can potentially bind to more than one enzyme species, E and E·SAM. The kinetic cooperativity observed for poor, non-native acyl-ACP substrates raise an important question: *why do poor substrates populate less favored kinetic paths and thus display a nonhyperbolic kinetic response?* Perhaps E·acyl-ACP complex is less stable for a poor acyl-ACP substrate? If E·acyl-ACP were unstable or short-lived, then E·SAM would accumulate in solution. Acyl-ACP binding to E·SAM would populate alternative, less favored paths for AHL synthesis (Figure 7A) and thus form the basis of kinetic cooperativity observed for these substrates.

The acyl carrier protein is an all α-helical, four-helix protein with the acyl chain sequestered in a hydrophobic tunnel between helices II and IV. The dynamic, acyl carrier protein offers some unique structural features that allow this protein to interact with a wide-range of partner enzymes in multiple metabolic pathways in vivo. A number of acyl-ACP structures both as an apo-structure and in complex with a partner enzyme have been published.[62−68] Acyl-ACP crystal structures show that the hydrophobic tunnel is plastic, and binding of the fatty acyl-chain can expand the internal cavity volume to about 164 Å^3 for decanoyl-ACP relative to apo-ACP.[62−65] The phosphopantetheine moiety is partially buried inside this core to different extents depending on the acyl-ACP, which would give
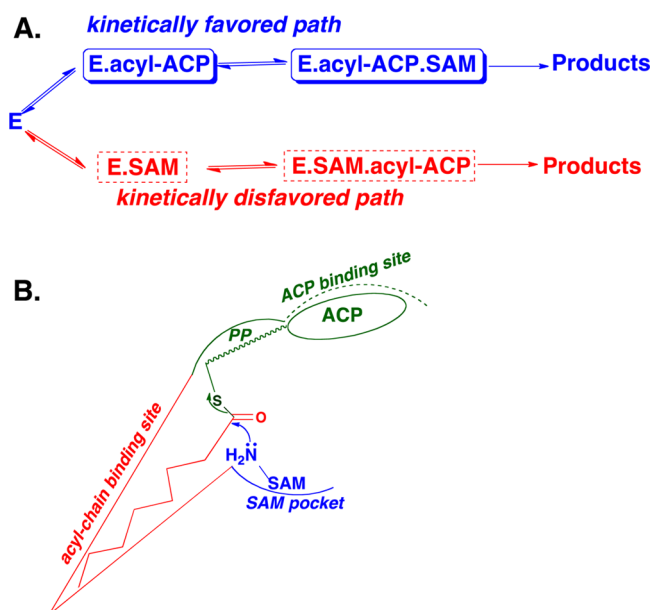
Figure 7. Native acyl-ACP substrate recognition by BmaI1. (A) Favored versus disfavored paths for AHL synthesis. The favored path is highlighted in blue and the disfavored path is in red. Productive and nonproductive enzyme−substrate complexes are represented by solid (blue) and dotted (red) rectangles, respectively. (B) A cartoon diagram representing a stable and productive [BmaI1·acyl-ACP·SAM] ternary complex. Acyl-chain, ACP, and SAM binding pockets in BmaI1 are represented in red, green, and blue colors, respectively. PP in this figure refers to the phosphopantetheine linker. For octanoyl-ACP, the thioester acyl carbonyl and SAM amine are locked in optimal conformation to facilitate acylation. A nonoptimal fit for non-native acyl-ACP substrates in BmaI1 active site should affect enzyme−substrate ternary complex stability, which decreases the catalytic constant and overall catalytic efficiencies for these substrates relative to octanoyl-ACP.

a unique surface contour for each acyl-ACP. Perhaps this forms an important part of the recognition surface that promotes specificity in its interactions with the partner enzyme? Once substrate-specific recognition is achieved, protein−protein interactions between ACP and a partner enzyme will mediate the reporting of the acyl-chain from acyl-ACP to the enzyme active site. A recently published report on FabA-acyl-ACP cross-linked structure suggests that the switch-blade release of the acyl-chain from acyl-ACP is a multistep process that begins with electrostatic binding interactions between negatively charged phosphopantetheine and a positively charged basic patch in FabA. Salt-bridges between ACP helix II and R132, K161 amino acid residues of FabA form to anchor the ES complex and enzyme-assisted movement of ACP helix III facilitates acyl-chain reporting to acyl-chain binding pocket in FabA.[66,69] If BmaI1 specifically recognizes octanoyl-ACP surface contour, then an altered recognition surface between BmaI1 and a non-native acyl-ACP substrate could potentially influence the rate of acyl-chain release, which could also affect the formation of a stable and productive E·acyl-ACP complex necessary to progress the AHL synthesis reaction along the kinetically preferred pathway.

FabA·acyl-ACP cocrystal structures show that acyl-chain release from acyl-ACP is enzyme dependent.[66] Therefore, specificity in enzyme-acyl-ACP substrate recognition should play a major role in this chain-flipping event. For a poor substrate, the lack of such specific interactions in the E·acyl-

ACP complex might hinder acyl-chain flipping or alternatively, the acyl-chain could be unstable when bound at the BmaI1 active site. In that instance, one could envision that the acyl-chain will be sequestered back between ACP helices II and IV thereby promoting the dissociation of the E·acyl-ACP complex. When a good substrate such as octanoyl-ACP binds to BmaI1, specificity achieved in formation of the E·acyl-ACP complex must facilitate acyl-chain reporting to the enzyme acyl-chain pocket. This will further enhance the stability of ES complex and aid in anchoring the acyl-ACP substrate in a productive conformation, optimal for acylation. A productive E·acyl-ACP complex would entail precise positioning of the thioester acyl carbonyl (acyl-donor) and SAM amine (acyl-acceptor) moieties to form a productive E·acyl-ACP·SAM ternary complex, conducive for acylation (Figure 7B).

We observed standard Michaelis−Menten response with octanoyl-ACP, hexanoyl-ACP, and decanoyl-ACP substrates (Figure 5). The close structural similarity of hexanoyl-ACP and decanoyl-ACP with octanoyl-ACP suggests that these substrates must be able to form a relatively stable E·acyl-ACP complex. Since k_{cat} and K_m for hexanoyl-ACP is similar to octanoyl-ACP, this indicates that a two-carbon shorter acyl-chain packs reasonably well compared to the two-carbon longer chain in the BmaI1 acyl-chain binding pocket. Although we observed a hyperbolic response for decanoyl-ACP, the reduced k_{cat} and higher K_m for this substrate relative to hexanoyl-ACP suggest that E·decanoyl-ACP is in a less productive conformation (the acyl-chain not anchored optimally for acylation) compared to E·hexanoyl-ACP. For poor substrates such as butyryl-ACP and octanoyl-CoA, the lag phase in substrate velocity curves observed at low substrate concentration hints that E·butyryl-ACP and E·octanoyl-CoA complex is less stable favoring the dissociation of this complex. MD simulations of acyl-ACPs suggest that the tip of the acyl-chain attempts to reach the bottom of hydrophobic cavity formed between helices II and IV of the ACP.[65] Therefore, a four-carbon shorter acyl-chain in butyryl-ACP should possess higher conformational mobility in BmaI1 acyl-chain binding pocket promoting the dissociation of E·butyryl-ACP complex. For the octanoyl-CoA substrate, the lack of ACP moiety should severely impair the formation of a productive ES complex. In short, hexanoyl-ACP and decanoyl ACP (substrates that closely resemble the octanoyl-ACP structure) can form a stable ES complex, but in a less productive mode for acylation. On the other hand, butyryl-ACP and octanoyl-CoA (substrates that possess larger structural deviations from octanoyl-ACP) can form neither stable nor productive ES complex. It seems that only the native acyl-ACP substrate can form both stable and productive ES complex, and therefore AHL synthesis rates with the octanoyl-ACP substrate are significantly higher than non-native acyl-ACP substrates. Cocrystallization of inert acyl-ACP analogues carrying native and non-native acyl-chains and SAM with BmaI1 is in progress to further understand structural differences between BmaI·(native)acyl-ACP·SAM and BmaI1·(non-native)acyl-ACP·SAM ternary complexes. In conclusion, our data suggest that recognition of native acyl-ACP substrate by BmaI1 is achieved through the formation of a stable and productive E·acyl-ACP·SAM ternary complex. Non-native acyl-donor substrates unable to form tight E·acyl-ACP·SAM ternary complexes are thus effectively discriminated by the enzyme. These results offer insights into understanding the molecular basis of tight signal specificity observed in *B. mallei* quorum sensing.

ASSOCIATED CONTENT

S Supporting Information

Mass-spectra of ACP and its derivatives. This material is available free of charge via the Internet at http://pubs.acs.org.

AUTHOR INFORMATION

Corresponding Author

*Phone: 208-426-1423. E-mail: rajnagarajan@boisestate.edu.

Present Address

§X.P.: Biomolecular Research Center, Boise State University, 1910 University Drive, Boise, Idaho 83725.

ABBREVIATIONS USED

ACP, acyl carrier protein; AHL, acyl-homoserine lactone; MTA, methyl thioadenosine; C8-HSL, octanoyl-homoserine lactone; AHL synthase, acyl-homoserine lactone synthase; acyl-ACP, acyl–acyl carrier protein; SAM, S-adenosyl-L-methionine; B-PER, bacterial protein extraction reagent; DCPIP, dichlorophenolindophenol; HEPES, (4-(2-hydroxyethyl)-1-piperazineethanesulfonic acid; Tris, tris(hydroxymethyl)-aminomethane; Q-TOF, quadrupole-time-of-flight; ESI, electrosprayionization; C4ACP, butyryl-ACP; C6ACP, hexanoyl-ACP; C8ACP, octanoyl-ACP; C10ACP, decanoyl-ACP; C8CoA, octanoyl-CoA; 3′5-ADP, 3′5′-adenosinediphosphate; IPTG, isopropyl-β-D-thiogalactoside

REFERENCES

(1) Davies, D. G., Parsek, M. R., Pearson, J. P., Iglewski, B. H., Costerton, J. W., and Greenberg, E. P. (1998) The involvement of cell-to-cell signals in the development of a bacterial biofilm. *Science 280*, 295–298.

(2) More, M. I., Finger, L. D., Stryker, J. L., Fuqua, C., Eberhard, A., and Winans, S. C. (1996) Enzymatic synthesis of a quorum-sensing autoinducer through use of defined substrates. *Science 272*, 1655–1658.

(3) Bassler, B. L. (2002) Small talk: cell-to-cell communication in bacteria. *Cell. 109*, 421–424.

(4) Huber, B., Riedel, K., Hentzer, M., Heydorn, A., Gotschlich, A., Givskov, M., Molin, S., and Eberl, L. (2001) The cep quorum-sensing system of *Burkholderia cepacia* H111 controls biofilm formation and swarming motility. *Microbiology 147*, 2517–2528.

(5) Passador, L., Cook, J. M., Gambello, M. J., Rust, L., and Iglewski, B. H. (1993) Expression of *Pseudomonas aeruginosa* virulence genes requires cell-to-cell communication. *Science 55* (260), 1127–1130.

(6) Smith, R. S., and Iglewski, B. H. (2003) *Pseudomonas aeruginosa* quorum sensing as a potential antibiotic target. *J. Clin. Invest. 112*, 1460–1465.

(7) Mattmann, M. E., and Blackwell, H. E. (2010) Small molecules that modulate quorum sensing and control virulence in *Pseudomonas aeruginosa*. *J. Org. Chem. 75* (20), 6737–6746.

(8) Ulrich, R. L., Deshazer, D., Hines, H. B., and Jeddeloh, J. A. (2004) Quorum sensing: a transcriptional regulatory system involved in the pathogenicity of *Burkholderia mallei*. *Infect. Immun. 72*, 6589–6596.

(9) Bobrov, A. G., Bearden, S. W., Fetherston, J. D., Khweek, A. A., Parrish, K. D., and Perry, R. D. (2007) Functional quorum sensing systems affect biofilm formation and protein expression in *Yersinia pestis*. *Adv. Exp. Med. Biol. 603*, 178–191.

(10) Sokol, P. A., Malott, R. J., Riedel, K., and Eberl, L. (2007) Communication systems in the genus Burkholderia: global regulators and targets for novel antipathogenic drugs. *Future Microbiol. 2*, 555–563.

(11) Lin, H. (2011) S-Adenosylmethionine-dependent alkylation reactions: When are radical reactions used? *Bioorg. Chem. 39*, 161–170.

(12) Hanzelka, B. L., and Greenberg, E. P. (1996) Quorum sensing in *Vibrio fischeri*: evidence that S-adenosylmethionine is the aminoacid substrate for autoinducer synthesis. *J. Bacteriol. 178*, 5291–5294.

(13) Fast, W., and Tipton, P. A. (2012) The enzymes of bacterial census and censorship. *Trends Biochem. Sci. 37* (1), 7–14.

(14) Parsek, M. R., Val, D. L., Hanzelka, B. L., Cronan, J. E., Jr, and Greenberg, E. P. (1999) Acyl- homoserine-lactone quorum-sensing signal generation. *Proc. Natl. Acad. Sci. U.S.A. 96*, 4360–4365.

(15) Raychaudhuri, A., Jerga, A., and Tipton, P. A. (2005) Chemical mechanism and substrate specificity of RhlI, an acylhomoserine lactone synthase from *Pseudomonas aeruginosa*. *Biochemistry 44*, 2974–2981.

(16) Raychaudhuri, A., Tullock, A., and Tipton, P. A. (2008) Reactivity and reaction order in acylhomoserine lactone formation by *Pseudomonas aeruginosa* RhlI. *Biochemistry 47* (9), 2893–2898.

(17) Parsek, M. R., Schaefer, A. L., and Greenberg, E. P. (1997) Analysis of random and site-directed mutations in RhlI, a *Pseudomonas aeruginosa* gene encoding an acyl homoserine lactone synthase. *Mol. Microbiol. 26*, 301–310.

(18) Brader, G., Sjoblom, S., Hyytiainen, H., Sims-Huopaniemi, K., and Palva, E. T. (2005) Altering substrate chain length specificity of an acylhomoserine lactone synthase in bacterial communication. *J. Biol. Chem. 280* (11), 10403–10409.

(19) Gould, T. A., Herman, J., Krank, J., Murphy, R. C., and Churchill, M. E. A. (2006) Specificity of acyl-homoserine lactone synthases examined by mass spectrometry. *J. Bacteriol. 188*, 773–783.

(20) Watson, W. T., Minogue, T. D., Val, D. L., Bodman, S. B., and Churchill, M. E. A. (2002) Structural basis and specificity of acyl-homoserine lactone signal production in bacterial quorum sensing. *Mol. Cell 9*, 685–694.

(21) Gould, T. A., Schweizer, H. P., and Churchill, M. E. A. (2004) Structure of the Pseudomonas aeruginosa acyl-homoserine lactone synthase LasI. *Mol. Microbiol. 53*, 1135–1146.

(22) Churchill, M. E. A, and Chen, L. (2011) Structural basis of acyl-homoserine lactone-dependent signaling. *Chem. Rev. 111*, 68–85.

(23) Waag, D., and Deshazer, D. (2005) Glanders: new insights into an old disease, *Biological Weapons Defense: Infectious Disease and Counterbioterrorism*, pp 209–237, Humana Press, Totowa, NJ.

(24) Whitlock, G. C., Estes, D. M., and Torres, A. G. (2007) Glanders: off to the races with *Burkholderia mallei*. *FEMS Microbiol. Lett. 277*, 115–122.

(25) Duerkop, B. A., Herman, J. P., Ulrich, R. L., Churchill, M. E. A., and Greenberg, E. P. (2008) The *Burkholderia mallei* BmaR3-BmaI3 quorum-sensing system produces and responds to N-3-hydroxy-octanoyl homoserinelactone. *J. Bacteriol. 190* (14), 5137–5141.

(26) Duerkop, B. A., Ulrich, R. L., and Greenberg, E. P. (2007) Octanoyl-homoserine lactone is the cognate signal for *Burkholderia mallei* BmaR1-BmaI1 quorum sensing. *J. Bacteriol. 189*, 5034–5040.

(27) Majerczyk, C., Kinman, L., Han, T., Bunt, R., and Greenberg, E. P. (2013) Virulence of *Burkholderia mallei* quorum-sensing mutants. *Infect. Immun. 81* (5), 1471–1478.

(28) Hoang, T. T., Sullivan, S. A., Cusick, J. K., and Schweizer, H. P. (2002) Beta-ketoacyl acyl carrier protein reductase (FabG) activity of the fatty acid biosynthetic pathway is a determining factor of 3-oxo-homoserine lactone acyl chain lengths. *Microbiology 148* (12), 3849–3856.

(29) Chung, H., Goo, E., Yu, S., Choi, O., Lee, J., Kim, J., Kim, H., Igarashi, J., Suga, H., Moon, J. S., Hwang, I., and Rhee, S. (2011)

Small-molecule inhibitor binding to an N-acyl-homoserine lactone synthase. *Proc. Natl. Acad. Sci. U.S.A.* 108 (29), 12089–12094.

(30) Christensen, Q. H., Grove, T. L., Booker, S. J., and Greenberg, E. P. (2013) A high-throughput screen for quorum sensing inhibitors that target acyl-homoserine lactone synthases. *Proc. Natl. Acad. Sci. U.S.A.* 110 (34), 13815–13820.

(31) Rock, C. O., and Cronan, J. E. (1980) Improved purification of acyl carrier protein. *Anal. Biochem.* 102 (2), 362–364.

(32) Cronan, J. E., and Thomas, J. (2009) Bacterial fatty acid synthesis and its relationships with polyketide synthetic pathways. *Methods Enzymol.* 459, 395–433.

(33) Thomas, J., and Cronan, J. E. (2005) The enigmatic acyl carrier protein phosphodiesterase of *Escherichia coli*: genetic and enzymological characterization. *J. Biol. Chem.* 280 (41), 34675–34683.

(34) Keating, D. H., Carey, M. R., and Cronan, J. E. (1995) The unmodified (apo) form of Escherichia coli acyl carrier protein is a potent inhibitor of cell growth. *J. Biol. Chem.* 270 (38), 22229–22235.

(35) Quadri, L. E., Weinreb, P. H., Lei, M., Nakano, M. M., Zuber, P., and Walsh, C. T. (1998) Characterization of Sfp, a *Bacillus subtilis* phosphopantetheinyl transferase for peptidyl carrier protein domains in peptide synthetases. *Biochemistry* 37, 1585–1595.

(36) La Clair, J. J., Foley, T. L., Schegg, T. R., Regan, C. M., and Burkart, M. D. (2004) Manipulations of carrier proteins in antibiotic synthesis. *Chem. Biol.* 11 (2), 195–201.

(37) Cleland, W. W. (1979) Statistical analysis of enzyme data. *Methods Enzymol.* 63, 103–108.

(38) Christensen, Q. H., and Cronan, J. E. (2010) Lipoic acid synthesis: A new family of octanoyltransferases generally annotated as lipoate protein ligases. *Biochemistry* 49 (46), 10024–10036.

(39) Chemler, J. A., Buchholz, T. J., Geders, T. W., Akey, D. L., Rath, C. M., Chlipala, G. E., Smith, J. L., and Sherman, D. H. (2012) Biochemical and structural characterization of germicidin synthase: analysis of a type III polyketide synthase that employs acyl-ACP as a starter unit donor. *J. Am. Chem. Soc.* 134 (17), 7359–7366.

(40) Borgaro, J. G., Chang, A., Machutta, C. A., Zhang, X., and Tonge, P. J. (2011) Substrate recognition by β-ketoacyl-ACP synthases. *Biochemistry.* 50 (49), 10678–10686.

(41) Broadwater, J. A., and Fox, B. G. (1999) Spinach holo-acyl carrier protein: Overproduction and phosphopantetheinylation in *Escherichia coli* BL21(DE3), in vitro acylation and enzymatic desaturation of histidine-tagged isoform I. *Protein Expression Purif.* 15, 314–326.

(42) Yu, X., Liu, T., Zhu, F., and Khosla, C. (2011) In vitro reconstitution and steady-state analysis of the fatty acid synthase from *Escherichia coli*. *Proc. Natl. Acad. Sci. U.S.A.* 108 (46), 18643–18648.

(43) Koppish, A. T., and Khosla, C. (2003) Structure-based mutagenesis of the malonyl-CoA:Acyl carrier protein transacylase from *Streptomyces coelicolor*. *Biochemistry* 42, 11057–11064.

(44) Flugel, R. S., Hwangbo, Y., Lambalot, R. H., Cronan, J. E., and Walsh, C. . (1999) Holo-(acyl carrier protein) synthase and phosphopantetheinyl transferase transfer in *Escherichia coli*. *J. Biol. Chem.* 275 (2), 959–968.

(45) Copeland, R. A. (2000) Enzyme Reactions with multiple substrates, Enzymes, 2nd ed., pp 350–367, Wiley-VCH, New York.

(46) Cleland, W. W., and Cook, P. F. (2007) *Enzyme Kinetics & Mechanism*, Garland Science, New York, pp 59–204.

(47) Cleland, W. W. (1963) The kinetics of enzyme-catalyzed reactions with two or more substrates or products: Prediction of intial velocity and inhibition patterns by inspection. *Biochim. Biophys. Acta* 67, 188–196.

(48) Kaiser, P. M. (1980) Substrate inhibition as a problem of non-linear steady state kinetics with monomeric enzymes. *J. Mol. Catal.* 8, 431–442.

(49) Porter, C. M., and Miller, B. G. (2012) Cooperativity in monomeric enzymes with single ligand-binding sites. *Bioorg. Chem.* 43, 44–50.

(50) Frieden, C. (1970) Kinetic aspects of regulation of metabolic processes: The hysteretic enzyme concept. *J. Biol. Chem.* 245 (21), 5788–5799.

(51) Gol'dshtein, B. N., and Vol'kenshtein, M. V. (1972) Cooperativity in two-substrate reactions. *Mol. Biol.* 5 (4), 441–449.

(52) Ainslie, G. R., Shill, J. P., and Neet, K. E. (1972) Transients and cooperativity: A slow transition model for relating transients and cooperative kinetics of enzymes. *J. Biol. Chem.* 247 (21), 7088–7096.

(53) Frieden, C. (1979) Slow transitions and hysteretic behavior in enzymes. *Annu. Rev. Biochem.* 48, 471–489.

(54) Neet, K. E., and Ainslie, G. R. (1980) Hysteretic enzymes. *Methods Enzymol.* 64, 192–226.

(55) Liu, S., Ammirati, M. J., Song, X., Knafels, J. D., Zhang, J., Greasley, S. E., Pfefferkorn, J. A., and Qiu, X. (2012) Insights into mechanism of glucokinase activation: observation of multiple distinct protein conformations. *J. Biol. Chem.* 287 (17), 13598–13610.

(56) Pettersson, G. (1986) Mechanistic origin of the sigmoidal rate behavior of glucokinase. *Biochem, J.* 233, 347–350.

(57) Storer, A. C., and Cornish-Bowden, A. (1977) Kinetic evidence for a 'mnemonical' mechanism for rat liver glucokinase. *Biochem. J.* 165, 61–69.

(58) Ricard, J., Meunier, J.-C., and Buc, J. (1974) Regulatory behavior of monomeric enzymes. *Eur. J. Biochem.* 49, 195–208.

(59) Pettersson, G. (1986) Mechanistic origin of the sigmoidal rate behavior of glucokinase. *Biochem. J.* 233, 347–350.

(60) Ferdinand, W. (1966) Interpretation of non-hyperbolic rate curves for two-substrate enzymes. *Biochem. J.* 98, 278–283.

(61) Kumar, S., Adediran, S. A., Nukaga, M., and Pratt, R. F. (2004) Kinetics of turnover of cefotaxime by the *Enterobacter cloacae* P99 and GC1 β-lactamases: Two free enzyme forms of the P99 β-lactamase detected by a combination of pre- and post-steady state kinetics. *Biochemistry.* 43, 2664–2672.

(62) Roujeinikova, A., Simon, W. J., Gilroy, J., Rice, D. W., Rafferty, J. B., and Slabas, A. R. (2007) Structural studies of fatty acyl-(acyl carrier protein) thioesters reveal a hydrophobic binding cavity that can expand to fit longer substrates. *J. Mol. Biol.* 365, 135–145.

(63) Roujeinikova, A., Baldock, C., Simon, W. J., Gilroy, J., Baker, P. J., Stuitje, A. R., Rice, D. W., Slabas, A. R., and Rafferty, J. B. (2002) X-ray crystallographic studies on butyryl-ACP reveal flexibility of the structure around a putative acyl chain binding site. *Structure* 10, 825–835.

(64) Upadhyay, S. K., Misra, A., Srivastava, R., Surolia, N., Surolia, A., and Sundd, M. (2009) Structural insights into the acyl intermediates of the *Plasmodium falciparum* fatty acid synthesis pathway: The mechanism of expansion of the acyl carrier protein core. *J. Biol. Chem.* 284 (33), 22390–22400.

(65) Chan, D. I., Stockner, T., Tieleman, D. P., and Vogel, H. J. (2008) Molecular dynamics simulations of the apo-, holo- and acyl-forms of *Escherichia coli* acyl carrier protein. *J. Biol. Chem.* 283 (48), 33620–33629.

(66) Nguyen, C., Haushalter, R. W., Lee, J. D., Markwick, P. R.L., Bruegger, J., Caldara-Festin, G., Finzel, K., Jackson, D. R., Ishikawa, F., O'Dowd, B., McCammon, A., Opella, S. J., Tsai, S.-C., and Burkart, M. D. (2014) Trapping the dynamic acyl carrier protein in fatty acid biosynthesis. *Nature* 505, 427–431.

(67) Masoudi, A., Raetz, C. R. H., Zhou, P., and Pemble, C. W., IV (2014) Chasing acyl carrier protein through a catalytic cycle of lipid A production. *Nature* 505, 422–426.

(68) Agarwal, V., Lin, S., Lukk, T., Nair, S. K., and Cronan, J. E. (2012) Structure of the enzyme-acyl carrier protein (ACP) substrate gatekeeper complex required for biotin synthesis. *Proc. Natl. Acad. Sci. U.S.A.* 109 (43), 17406–17411.

(69) Cronan, J. E. (2014) The chain-flipping mechanism of ACP (acyl carrier protein)-dependent enzymes appears universal. *Biochem. J.* 460, 157–163.